OPEN ACCESS

Structural fluctuations and quantum transport through DNA molecular wires: a combined molecular dynamics and model Hamiltonian approach

New Journal of Physics
The open-access journal for physics

Structural fluctuations and quantum transport through DNA molecular wires: a combined molecular dynamics and model Hamiltonian approach

R Gutiérrez[1,4], R Caetano[2], P B Woiczikowski[3], T Kubar[3], M Elstner[3] and G Cuniberti[1]

[1] Institute for Materials Science and Max Bergmann Center of Biomaterials, Dresden University of Technology, 01062 Dresden, Germany
[2] Instituto de Fisica, Universidade Federal de Alagoas, Maceio, AL 57072-970, Brazil
[3] Institute for Physical Chemistry, Karlsruhe Institute of Technology, 76131 Karlsruhe, Germany
E-mail: rafael.gutierrez@tu-dresden.de

New Journal of Physics **12** (2010) 023022 (16pp)
Received 30 September 2009
Published 16 February 2010
Online at http://www.njp.org/
doi:10.1088/1367-2630/12/2/023022

Abstract. Charge transport through a short DNA oligomer (Dickerson dodecamer (DD)) in the presence of structural fluctuations is investigated using a hybrid computational methodology based on a combination of quantum mechanical electronic structure calculations and classical molecular dynamics (MD) simulations with a model Hamiltonian approach. Based on a fragment orbital description, the DNA electronic structure can be coarse-grained in a very efficient way. The influence of dynamical fluctuations, arising either from the solvent fluctuations or from base-pair vibrational modes, can be taken into account in a straightforward way through the time series of the effective DNA electronic parameters, evaluated at snapshots along the MD trajectory. We show that charge transport can be promoted through the coupling to solvent fluctuations, which gate the on-site energies along the DNA wire.

[4] Author to whom any correspondence should be addressed.

Contents

1. Introduction

The electrical response of DNA oligomers to an applied voltage is a highly topical issue that has attracted the attention of scientists belonging to different research communities. Experimentally, a variety of results have been achieved predicting DNA to be an insulator [1], a semiconductor [2, 3] or a metallic-like system [4, 5]. This fact hints not only at the difficulties encountered in carrying out well-controlled single-molecule experiments but also at the dramatic sensitivity of charge migration through DNA molecules to intrinsic, system-related, or extrinsic, set-up-mediated factors: the specific base pair sequence, internal vibrational excitations, solvent fluctuations, the electrode–molecule interface topology, among others. As a result, the theoretical modeling of DNA quantum transport remains a very challenging issue that has been approached from many different sides, see e.g. [6]–[9] for recent reviews.

Most of the models originally proposed to deal with *charge transport* through DNA oligomers started from a static picture of the DNA structure and of the corresponding electronic properties, see e.g. [10]–[13]. However, hole transfer experiments [14]–[20] as well as related theoretical work [21]–[25] in the chemical physics community strongly suggested that charge migration through DNA oligomers can be understood only in the context of a *dynamical approach* that includes the coupling of the electronic system to conformational degrees of freedom, resulting in fully or partially incoherent charge propagation. Indeed, strong conformational dynamics and a related spectrum of different time scales seem to be ubiquitous for biomolecules, as shown, for example, in the modulation of the kinetics of electron transfer during the early stages of the photosynthetic reaction cycle [26, 27], by the analysis of dispersed kinetics [28]–[30] or by fluorescence correlation spectroscopy [31]. In light of these experimental and theoretical studies, it seems natural to expect that dynamical effects would also play a determining role in charge transport processes for biomolecular systems like DNA contacted by metallic electrodes. However, the relatively small number of well-controlled electrical transport experiments [3]–[5], [32] makes it difficult to arrive at a conclusive answer about the degree to which dynamical effects dominate charge transport, although the strong temperature dependence of the electrical current observed, for example, in [5] suggests that the influence is important. Several theoretical studies have considered the influence of structural fluctuations on electrical transport from different perspectives [33]–[41]; a realistic inclusion of

the influence of dynamical effects on the transport properties can, however, only be achieved, in our view, via hybrid methodologies combining a reliable description of the biomolecular dynamics and electronic structure with quantum transport calculations. *Ab initio* approaches for static biomolecular structures can provide a very valuable starting point for the parameterization of model Hamiltonians [42]–[50]; however, a full first-principle treatment of both the dynamics and electronic structure lies outside the capabilities of state-of-the-art methodologies.

In this paper, we will elaborate on a recent study on homogeneous DNA sequences [36] by addressing in detail some methodological issues. Our focus will be on the Dickerson dodecamer (DD) [51] with the sequence 5′-CGCGAATTCGCG-3′ for which the effect of the dynamical fluctuations becomes very clear. Our approach combines classical molecular dynamics (MD) simulations with electronic structure calculations to provide a realistic starting point for the description of the influence of structural fluctuations on the electronic structure of a biomolecule. Further, the information drawn from such calculations will be used to formulate low-dimensional effective Hamiltonians to describe charge transport. A central point is the use of the concept of fragment orbitals [24], [52]–[54], which allows for a very efficient and flexible mapping of the electronic structure of a complex system onto a much simpler effective model. Taking a single base pair as a fragment and considering only one relevant fragment orbital per base pair, we end up in a tight-binding Hamiltonian for a linear chain where both on-site energies $\epsilon_j(t)$ and electronic coupling terms $V_{j,j+1}(t)$ are time-dependent variables:

$$H = \sum_j \epsilon_j(t) d_j^\dagger d_j + \sum_j V_{j,j+1}(t)\,(d_j^\dagger d_{j+1} + \text{h.c.}). \tag{1}$$

The dynamic information provided in this way builds the starting point of our treatment of quantum transport through biomolecular wires. In the next section, we briefly describe the computational methodology used to obtain the effective electronic parameters of the model Hamiltonian, which will then be introduced in section 3, where we also illustrate how to relate the Hamiltonian of equation (1) to a different model describing the coupling of a time-independent electronic system to a bosonic bath. Further, expressions for the electrical current as well as the relation between the auto-correlation function of the on-site energy fluctuations and the spectral density of the bosonic bath will be derived. Finally, in section 3, we discuss the transport properties of the DD in vacuum and in the presence of a solvent. We stress that in contrast to other models that explicitly contain the coupling to vibrational excitations or to an environment [38]–[41], [55] at the price of introducing several free parameters, our methodology potentially contains the full dynamical complexity of the biomolecule as obtained from the MD simulations. One main advantage of our approach is the possibility of progressively improving the degree of coarse-graining by an appropriate re-definition of the molecular fragments.

2. MD and model Hamiltonian formulation

2.1. Computational methodology

We will first give an overview of the fragment-orbital approach used in our computations; further details can be found elsewhere [52, 53, 56].

The core of our method is based on a combination of a self-consistent-charge density-functional tight-binding approach (SCC-DFTB) and the fragment orbital concept [56]; both

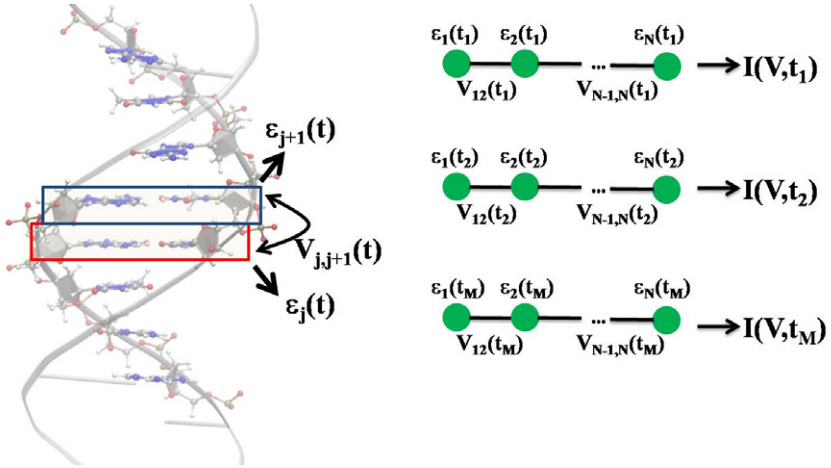

Figure 1. Left panel: schematic representation of the fragment orbital method used to perform a coarse-graining of the DNA electronic structure. A fragment consists of a single base pair (not including the sugar-phosphate backbones). As explained in the text, the hopping matrix elements $V_{j,j+1}$ between nearest-neighbor fragments are computed using the molecular orbital basis of the isolated base pairs. These calculations are then carried out at snapshots along the MD trajectory, hence leading to time-dependent electronic structure parameters. By keeping only one relevant orbital per fragment, the electronic structure can be mapped onto that of a linear chain (right panel). Transport observables can be computed at each simulation time step. Alternatively, the time dependence of the electronic structure (related to structural and solvent fluctuations) can be transferred to a bosonic bath as done in this paper.

are used to compute the electronic parameters $\epsilon_j(t)$ and $V_{j,j+1}(t)$ for the effective tight-binding model introduced in equation (1) in a very efficient way; see figure 1 for a schematic representation. The $V_{j,j+1}$ are calculated using the highest occupied molecular orbital Φ_i computed for isolated bases as $V_{j,j+1} = \langle \Phi_j | H | \Phi_{j+1} \rangle$, where the Φ_j's can be expanded in a valence atomic orbital basis η_μ on a given fragment: $\Phi_j = \sum_\mu c_\mu^j \eta_\mu$. The real expansion coefficients c_μ^j are obtained from calculations on isolated bases and stored for subsequent use to calculate $V_{j,j+1}$. Therefore, one can write

$$V_{j,j+1} = \sum_\mu \sum_\nu c_\mu^j c_\nu^{j+1} \langle \eta_\mu | H | \eta_\nu \rangle . \tag{2}$$

The Hamilton matrix in the atomic orbital basis $H_{\mu\nu} = \langle \eta_\mu | H | \eta_\nu \rangle$ evaluated using the SCC-DFTB Hamiltonian matrix is pre-calculated and stored, thus making this step extremely efficient, i.e. it can be calculated for geometry snapshots generated by a classical MD simulation even for several nanoseconds. Additionally, the minimal linear combination of atomic orbitals (LCAO) basis set used in the standard SCC-DFTB code has been optimized for the calculation of the hopping matrix elements [52, 53], and the results are in very good agreement with other approaches [43, 56]. Concerning now the coupling to the solvent, a hybrid quantum mechanics/molecular mechanics (QM/MM) approach has been used, and implemented in the SCC-DFTB code [57], leading to the following Hamiltonian matrix in the

valence atomic orbital basis η_ν:

$$H_{\mu\nu}^{\mathrm{QM/MM}} = H_{\mu\nu}^{\text{SCC-DFTB}} + \frac{1}{2}S_{\mu\nu}\left\{\sum_{\delta} Q_\delta\left(\frac{1}{R_{\alpha\delta}}+\frac{1}{R_{\beta\delta}}\right)+\sum_{A} Q_A\left(\frac{1}{r_{A\alpha}}+\frac{1}{r_{A\beta}}\right)\right\}. \tag{3}$$

Here, Q_δ are the Mulliken charges of the quantum-mechanical region and the Q_A are the charges in the MM region (backbone, counter-ions and water), $S_{\mu\nu}$ is the atomic orbital overlap matrix, $H_{\mu\nu}^{\text{SCC-DFTB}}$ is the corresponding zero-order Hamiltonian matrix and $R_{\alpha\delta}$ is the distance between the DNA atom where the AO orbital η_μ is located and the MM atom in the solvent with charge Q_δ. The last term explicitly takes into account the coupling to the environment (solvent). The ϵ_j and $V_{j,j\pm1}$ from equation (2) using equation (3) can now be calculated along the MD trajectories [37, 53]. The off-diagonal matrix elements strongly depend on structural fluctuations of the DNA base pairs, but they are only weakly affected by the solvent dynamics, the opposite holding for the on-site energies that are considerably modified by solvent fluctuations [37, 53]. The Fourier transform of the on-site energies auto-correlation function provides information about the spectral ranges that are more strongly contributing to the fluctuations of the electronic parameters, see also the next sections. Thus, we have found that the apparently most important modes are located around 1600 cm^{-1} corresponding to a base skeleton mode and at 800 cm^{-1} related to the water modes [53]. Both contributions modulate the on-site energies significantly on a short time scale and a long time scale of about 1 ps, respectively.

2.2. *Model Hamiltonian for electronic transport*

Using equation (1) directly for quantum transport calculations may mask to some degree different contributions (solvent, base dynamics) to charge propagation through the DNA π-stack. Moreover, since equation (1) contains random variables through the time series, we are confronted with the problem of dealing with charge transport in a stochastic Hamiltonian. This is a more complex task that has been addressed, for example, in the context of exciton transport [58]–[61], but also to some degree in electron transfer theories [62]–[64]. Here, we adopt a different point of view and formulate a model Hamiltonian, where the relevant electronic system, in this case the fragment orbital-derived effective DNA electronic system, is coupled explicitly to a bosonic bath. The latter will encode through its spectral density the dynamical information drawn from the MD simulations on internal base dynamics as well as solvent fluctuations. The Hamiltonian can be written in the following way:

$$H = \sum_j \langle\epsilon_j\rangle_t\, d_j^\dagger d_j - \sum_j \langle V_{j,j+1}\rangle_t\,(d_j^\dagger d_{j+1} + \text{h.c.}) + H_{\text{bath}} + H_{\text{el-bath}} + H_{\text{tunnel}} + H_{\text{leads}}, \tag{4}$$

$$H_{\text{bath}} = \sum_\alpha \Omega_\alpha B_\alpha^\dagger B_\alpha,$$

$$H_{\text{el-bath}} = \sum_{\alpha,j} \lambda_\alpha d_j^\dagger d_j (B_\alpha + B_\alpha^\dagger),$$

$$H_{\text{tunnel}} = \sum_{\mathbf{k},s,j}\left(t_{\mathbf{k}s,j} c_{\mathbf{k}s}^\dagger d_j + \text{h.c.}\right),$$

$$H_{\text{leads}} = \sum_{\mathbf{k},s} \epsilon_{\mathbf{k}s} c_{\mathbf{k}s}^\dagger c_{\mathbf{k}s}.$$

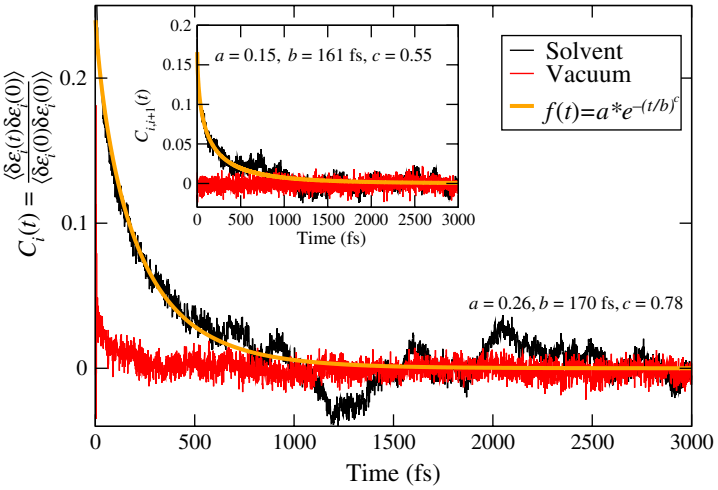

Figure 2. Normalized auto-correlation function [65] $C_i(t) = \langle \delta\epsilon_i(t)\delta\epsilon_i(0)\rangle / \langle \delta\epsilon_i^2 \rangle$ and averaged nearest-neighbor correlation function $C_{i,i+1}(t) = \langle \delta\epsilon_i(t)\delta\epsilon_{i+1}(0)\rangle / \langle \delta\epsilon_i \delta\epsilon_{i+1}\rangle$ (inset) of the on-site energy fluctuations. Solid lines are fits to stretched exponentials, which suggests the existence of different time scales, a typical situation in the dynamics of biomolecules [67]. On average, the decay of $C_{i,i+1}(t)$ occurs on a much shorter time scale than that of $C_i(t)$, so that our model will only include in a first approximation local fluctuations, see equation (5).

The time averages (over the corresponding time series) of the electronic parameters $\langle \epsilon_j \rangle_t$ and $\langle V_{j,j+1} \rangle_t$ have been split off to provide a zero-order Hamiltonian that contains dynamical effects in a mean-field-like level. The effect of the fluctuations around these averages is hidden in the vibrational bath, which is assumed to be a collection of a large ($N \to \infty$) number of harmonic oscillators in thermal equilibrium at temperature $k_B T$. The bath will be characterized by a spectral density $J(\omega)$, which can also be extracted from the MD simulations, as shown below and in [65]. Since we are interested in calculating the electrical response of the system, the charge-bath model has to also include the coupling of the system to electronic reservoirs (electrodes). The coupling to the electrodes will be treated in a standard way, using a tunneling Hamiltonian H_{tunnel} that describes the coupling to the s-lead with $s =$ left (L) or right (R). Later on, the so-called wide-band limit will be introduced (the corresponding electrode self-energies are purely imaginary and energy independent), thus reducing the electrode–DNA coupling to a single parameter.

The previous model relies on some basic assumptions that can be substantiated by the results of the MD simulations [53]: (i) the complex DNA dynamics can be well mimicked within the harmonic approximation by using a continuous vibrational spectrum; (ii) the simulations show that the local on-site energy fluctuations are much stronger in the presence of a solvent than those of the electronic hopping integrals (see also the end of the previous section), so that we assume that the bath is coupled only diagonally to the charge density fluctuations; (iii) fluctuations on different sites display rather similar statistical properties, so that the charge–bath coupling λ_α is taken to be independent of the site j. This latter approximation can be lifted by introducing additional site-non-local spectral densities $J_{j,j+1}(\omega)$; this, however, would make the theory more involved and less transparent. In figure 2, we show typical normalized auto-correlation functions of the on-site energy fluctuations for the DD in both solvent and vacuum

conditions as well as one case of off-diagonal correlations between nearest-neighbor site energies (inset). When speaking of simulations in vacuum conditions, we mean that the last term in equation (3) is left out. Also shown are fits to stretched exponentials, which are in general equivalent to a sum of simple exponential functions. This suggests the presence of different time scales and the nontrivial time dependence of the fluctuation dynamics. The fits become obviously less accurate at long times due to the reduced number of sampled data points with increasing time (the oscillatory behavior becomes stronger). From the figure we first see that the off-diagonal correlations decay on a much shorter time scale than the local ones, so that a first approximation to neglect them can be justified; further, the decay of the correlations for the vacuum simulations is considerably faster than in a solvent, indicating the strong influence of the latter in gating the electronic structure of the biomolecule. The corresponding correlation functions for the hopping integrals $V_{j,j+1}(t)$ (not shown) display even shorter relaxation times, so that the approximation $V_{j,j+1}(t) = \langle V_{j,j+1}(t)\rangle_t$ is enough for our purposes (the hopping integrals are self-averaging). We also mention that a stretched exponential behavior has also been investigated in a more general context for analyzing the influence of static and dynamic torsional disorder on the kinetics of charge transfer donor–bridge–acceptor systems [66].

In order to deal with the previous model, we first perform a polaron transformation of the Hamiltonian equation (4), using the generator $\mathcal{U} = \exp[\sum_{\ell,\alpha} g_\alpha d_\ell^\dagger d_\ell (B_\alpha^\dagger - B_\alpha)]$, which is nothing else than a shift operator of the harmonic oscillator equilibrium positions. The parameter $g_\alpha = \lambda_\alpha/\Omega_\alpha$ gives an effective measure of the electron–vibron coupling strength. Since we will work in the wide-band limit for the electrode self-energies, the renormalization of the tunneling Hamiltonian by a vibronic operator will be neglected. As a result, we obtain a Hamiltonian with decoupled electronic and vibronic parts and where the on-site energies are shifted as $\langle\epsilon_j\rangle_t \to \langle\epsilon_j\rangle_t - \int_0^\infty \mathrm{d}\omega J(\omega)/\omega$. However, as is well known [68], the retarded Green function of the system is now an entangled electronic–vibronic object that cannot be treated exactly; we thus decouple it in the approximate way [55, 69]:

$$\begin{aligned}\mathcal{G}_{nm}(t,t') &= -\mathrm{i}\theta(t-t')\left\langle\left[d_n(t)\mathcal{X}^\dagger(t), d_m^\dagger(t')\mathcal{X}(t')\right]_+\right\rangle \\ &\approx -\mathrm{i}\theta(t-t')\left\{\left\langle d_n(t)d_m^\dagger(t')\right\rangle\left\langle\mathcal{X}^\dagger(t)\mathcal{X}(t')\right\rangle + \left\langle d_m^\dagger(t')d_n(t)\right\rangle\left\langle\mathcal{X}(t')\mathcal{X}^\dagger(t)\right\rangle\right\} \\ &= \theta(t-t')\left\{G_{nm}^{>}(t,t')\mathrm{e}^{-\phi(t-t')} - G_{nm}^{<}(t,t')\mathrm{e}^{-\phi(t'-t)}\right\}, \qquad (5)\end{aligned}$$

$$\phi(t) = \sum_\alpha \left(\frac{\lambda_\alpha}{\Omega_\alpha}\right)^2 \left[(1+N_\alpha)\mathrm{e}^{-\mathrm{i}\Omega_\alpha t} + N_\alpha \mathrm{e}^{+\mathrm{i}\Omega_\alpha t}\right].$$

In this equation, $\theta(t-t')$ is the Heaviside function and the pure bosonic operator $\mathcal{X}(t) = \exp[\sum_\alpha g_\alpha(B_\alpha^\dagger - B_\alpha)]$. In the last row of equation (5), we can pass to the continuum limit and express $\phi(t)$ in terms of the bath spectral density $J(\omega)$ [70]:

$$\phi(t) = \frac{1}{\hbar}\int_0^\infty \mathrm{d}\omega \frac{J(\omega)}{\omega^2}\coth\frac{\hbar\omega}{k_\mathrm{B}T}(1-\cos\omega t) - \mathrm{i}\frac{1}{\hbar}\int_0^\infty \mathrm{d}\omega\frac{J(\omega)}{\omega^2}\sin\omega t. \qquad (6)$$

2.3. The electrical current

We derive in this section the expression we are going to use to calculate the electrical current through the DNA oligomer under study. The starting point is the well-known Meir–Wingreen

expression for the current from lead s [71]:

$$I_s = \frac{2e}{\hbar}\int \frac{\mathrm{d}E}{2\pi}\,\mathrm{Tr}\left\{\Sigma_s^<(E)G^>(E) - \Sigma_s^>(E)G^<(E)\right\}.$$

Now, we can exploit the decoupling approximation used in equation (5) together with the wide-band limit in the electrode–molecule coupling to write, for example, for the left electrode:

$$\Sigma_\mathrm{L}^<(E)G^>(E) = \int \frac{\mathrm{d}E'}{2\pi}\, f_\mathrm{L}(E)(1-f_\mathrm{R}(E'))t(E')\Phi(E-E'),$$

$$\Sigma_\mathrm{L}^>(E)G^<(E) = \int \frac{\mathrm{d}E'}{2\pi}\,(1-f_\mathrm{L}(E))\,f_\mathrm{R}(E')t(E')\Phi(E'-E),$$

$$\Phi(E) = \int \frac{\mathrm{d}t}{\hbar}\,\mathrm{e}^{(\mathrm{i}/\hbar)Et}\mathrm{e}^{-\phi(t)}.$$

Here, we have used the explicit expressions for the greater- and lesser-Green functions:

$$G_0^{>,<}(E) = G_0(E)(\Sigma_\mathrm{L}^{>,<}(E) + \Sigma_\mathrm{R}^{>,<}(E))G_0^\dagger(E), \tag{7}$$

the index 0 indicating that the vibrational degrees of freedom have already been decoupled. The transmission-like function $t(E)$ is given by $t(E) = \mathrm{Tr}\{G_0(E)\Gamma_\mathrm{L}G_0^\dagger(E)\Gamma_\mathrm{R}$. The retarded matrix Green function $G_0(E)$ is calculated without electron–bath coupling, but including the interaction with the electrodes: $G_0^{-1}(E) = E + \mathrm{i}\eta - H_0 + \mathrm{i}\Gamma_\mathrm{L} + \mathrm{i}\Gamma_\mathrm{R}$, with H_0 being the electronic part of the Hamiltonian of equation (4). Using these results, the right-going current can be written as

$$I_\mathrm{L} = \frac{2e}{\hbar}\int \frac{\mathrm{d}E}{2\pi}\int \frac{\mathrm{d}E'}{2\pi}\,t(E')\,\left\{f_\mathrm{L}(E)(1-f_\mathrm{R}(E'))\Phi(E-E') - (1-f_\mathrm{L}(E))\,f_\mathrm{R}(E')\Phi(E'-E)\right\}, \tag{8}$$

a similar expression holding for the left-going current, when the indices L and R are interchanged. The total current can be written in a symmetrized way: $I_\mathrm{T} = (I_\mathrm{L} - I_\mathrm{R})/2$. Note that the previous expression is similar to that obtained in the context of the $P(E)$ theory of Coulomb blockade, where the electromagnetic environment plays the role of the bosonic bath [70, 72]. By looking at equation (6), two limiting cases can immediately be obtained: the zero charge–bath coupling ($\phi = 0$), which implies $\Phi(E) = 2\pi\delta(E)$. In this limit, we recover the conventional expression for coherent transport, involving only the transmission function $t(E)$. In the high-temperature and/or strong coupling limit to the bath, a short-time expansion of $\phi_{sc}(t)$ can be performed, yielding

$$\phi_{sc}(t) = \frac{t^2}{2\hbar}\int_0^\infty \mathrm{d}\omega\, J(\omega)\coth\frac{\hbar\omega}{k_\mathrm{B}T} - \mathrm{i}\frac{t}{\hbar}\int_0^\infty \mathrm{d}\omega\frac{J(\omega)}{\omega} = \kappa_\mathrm{therm}t^2 - \mathrm{i}\frac{E_\mathrm{reorg}}{\hbar}t.$$

In the former expression, $\sqrt{\kappa_\mathrm{therm}}$ is related to an inverse decoherence time. In the high-temperature limit, $\kappa_\mathrm{therm} \sim k_\mathrm{B}T\,E_\mathrm{reorg}$. The Fourier transform of $\mathrm{e}^{-\phi_\mathrm{sc}(t)}$ can be calculated straightforwardly and gives

$$\Phi(E) = \sqrt{\frac{\pi}{\hbar^2\kappa_\mathrm{therm}}}\exp\left[-\frac{(E+E_\mathrm{reorg})^2}{4\hbar^2\kappa_\mathrm{therm}}\right].$$

Thus, the current calculated using equation (8) becomes a convolution of $t(E)$ with a Gaussian function. Note the similarity of this expression with the Franck–Condon factor appearing in the Marcus electron transfer theory.

2.4. Spectral density from MD

The next issue at stake is how to relate the bath spectral density $J(\omega)$ to the time series of the electronic parameters as obtained through the MD simulations. To illustrate this point, we will consider the simple case of a single level, whose site energy is a Gaussian random variable, coupled to left and right electrodes according to the Hamiltonian (we assume for simplicity that $\langle\epsilon(t)\rangle = 0$):

$$H = \delta\epsilon(t)d^{\dagger}d + H_{\text{tunnel}} + H_{\text{leads.}} \tag{9}$$

To deal with this problem, we may use equation of motion techniques for the retarded dot Green function $G(t,t') = -(\mathrm{i}/\hbar)\theta(t-t')\langle\{d(t), d^{\dagger}(t')\}\rangle$ in the time domain:

$$(\mathrm{i}\hbar\partial_t - \delta\epsilon(t))G(t,t') = \delta(t-t') + \sum_{\mathbf{k},\alpha} t^{\dagger}_{\mathbf{k},\alpha} G_{\mathbf{k}\alpha}(t,t'), \tag{10}$$

with $G_{\mathbf{k}\alpha}(t,t') = -(\mathrm{i}/\hbar)\theta(t-t')\langle c_{\mathbf{k},\alpha}(t), d^{\dagger}(t')\rangle$. A similar equation of motion for the latter function allows us to introduce the electrode self-energies:

$$\begin{aligned}(\mathrm{i}\hbar\partial_t - \delta\epsilon(t))G(t,t') &= \delta(t-t') + \int \mathrm{d}\tau\, \Sigma(t,\tau)G(\tau,t'),\\ \Sigma(t,\tau) &= \sum_{\mathbf{k},\alpha} |t_{\mathbf{k},\alpha}|^2 \mathrm{e}^{-\mathrm{i}\epsilon_{\mathbf{k},\alpha}t}.\end{aligned} \tag{11}$$

Note that the Green function thus obtained is still a random function, since no average over the random variable $\delta\epsilon(t)$ has as yet been performed. Using the wide-band limit in the lead self-energies $\Sigma_{\alpha}(t,t') = -\mathrm{i}\Gamma_{\alpha}\delta(t-t')$, we obtain, with $\Gamma = \Gamma_L + \Gamma_R$:

$$(\mathrm{i}\hbar\partial_t - \delta\epsilon(t) + \mathrm{i}\Gamma)G(t,t') = \delta(t-t'). \tag{12}$$

Introducing the time exponential $\mathcal{U}(t,t') = \exp(-(\mathrm{i}/\hbar)\int_{t'}^{t}\mathrm{d}s(\delta\epsilon(t) - \mathrm{i}\Gamma))$ allows us to write a closed solution for the dot Green function:

$$G(t,t') = -\frac{\mathrm{i}}{\hbar}\theta(t-t')\mathcal{U}(t,t'). \tag{13}$$

The average Green function over the random variable $\delta\epsilon(t)$ yields now in energy space:

$$\langle G(E)\rangle = -\frac{\mathrm{i}}{\hbar}\int_0^{\infty}\mathrm{d}t\,\mathrm{e}^{(\mathrm{i}/\hbar)E(t-t')}\left\langle\mathcal{U}(t-t')\right\rangle = -\mathrm{i}\int_0^{\infty}\mathrm{d}t\,\mathrm{e}^{(\mathrm{i}/\hbar)(E+\mathrm{i}\Gamma)(t-t')}\left\langle\mathrm{e}^{-(\mathrm{i}/\hbar)\int_{t'}^{t}\mathrm{d}s\delta\epsilon(s)}\right\rangle. \tag{14}$$

Performing now a cumulant expansion [73] of the averaged exponential and taking into account that cumulants higher than the second one exactly vanish due to the Gaussian nature of the fluctuations and to the fact that $\delta\epsilon(t)$ is a classical variable, we obtain (with $t' = 0$)

$$\langle G(E)\rangle = -\frac{\mathrm{i}}{\hbar}\int_0^{\infty}\mathrm{d}t\,\mathrm{e}^{(\mathrm{i}/\hbar)(E+\mathrm{i}\Gamma)t}\,\mathrm{e}^{-(1/\hbar^2)\int_0^t\mathrm{d}s\int_0^s\mathrm{d}s'\left\langle\delta\epsilon(s)\delta\epsilon(s')\right\rangle}, \tag{15}$$

which is the formally exact solution of the problem. We may now look at the same problem from a different point of view by considering *explicitly* the coupling of a single site with time-independent on-site energy to a continuum of vibrational excitations. Using the polaron transformation together with the approximations introduced at the beginning of section 2.2, we can write the retarded Green function as

$$G(E) = -\frac{\mathrm{i}}{\hbar}\int_0^{\infty}\mathrm{d}t\,\mathrm{e}^{(\mathrm{i}/\hbar)(E+\mathrm{i}\Gamma)t}\,\mathrm{e}^{-\phi(t)}, \tag{16}$$

where $\phi(t)$ has already been defined in equation (6). By comparison of equations (15) and (16), there must exist a relation between the (real) correlation function and the real part of $\phi(t)$. The latter can be rewritten in the following way:

$$\begin{aligned}\mathrm{Re}\,\phi(t) &= \frac{1}{\hbar}\int_0^\infty \mathrm{d}\omega\,\frac{J(\omega)}{\omega^2}\coth\frac{\hbar\omega}{k_\mathrm{B}T}(1-\cos\omega t)\\ &= \int_0^t \mathrm{d}s\int_0^s \mathrm{d}s'\left\{\frac{1}{\hbar}\int_0^\infty \mathrm{d}\omega\,J(\omega)\coth\frac{\hbar\omega}{k_\mathrm{B}T}\cos[\omega\,(s-s')]\right\},\end{aligned}$$

from which we conclude that

$$\left\langle\delta\epsilon(s)\delta\epsilon(s')\right\rangle = \hbar\int_0^\infty \mathrm{d}\omega\,J(\omega)\coth\frac{\hbar\omega}{k_\mathrm{B}T}\cos\left[\omega\,(s-s')\right].$$

From this, it follows, by inversion that,

$$J(\omega) = \frac{2}{\pi\hbar}\tanh\frac{\hbar\omega}{k_\mathrm{B}T}\int_0^\infty \mathrm{d}t\cos\omega t\,C(t) = \frac{2}{\pi\hbar}\tanh\frac{\hbar\omega}{k_\mathrm{B}T}j(\omega). \tag{17}$$

The previous result was obtained in [65] in the weak coupling, perturbative regime to the vibrational system; we have shown here that it can be extended also to the case of arbitrary coupling. Similar expressions could be derived for (spatially) non-local spectral densities.

2.5. Results

To illustrate our methodology, we have focused on DD, which has a non-homogeneous base sequence. In contrast to our previous study [36], where homogeneous DNA sequences were addressed like poly(G)-poly(C) and poly(A)-poly(T), the study of the DD nicely illustrates the role of the solvent fluctuations in gating the electronic structure. To study the effect of the conformational dynamics as well as the fluctuations of the environment on the charge transport properties, we have performed classical MD simulations using the AMBER-parm99 [74] force field with the parmBSC0 extension [75] as implemented in GROMACS [76] software package. The static geometries were built with 3DNA program [77], while the starting structures for the MD simulations were created using the make-na server [78]. After a standard heating procedure followed by a 1 ns equilibration phase, we performed 30 ns MD simulations with a time step of 2 fs. The simulations were carried out in a rectangular box with periodic boundary conditions and filled with 5500 TIP3P water molecules and 22 sodium counterions for neutralization. Snapshots of the molecular structures were saved every 1 ps, for which the charge transfer parameters were calculated with the methodology described in the previous sections. Upon mapping the electronic structure onto a linear chain as discussed in the former sections, we have first computed the time- and energy-dependent quantum-mechanical transmission function $T(E,t)$ by evaluating for every set of charge transfer parameters, i.e., at each simulation time step t, $\langle T(E,t)\rangle_t = (1/T_\mathrm{MD})\sum_j T(E,t_j)$. This quantity is expected to provide some qualitative insight into different factors affecting transport (solvent versus vacuum), but its use is restricted by the fact that for longer chains inelastic, fluctuation-mediated channels will play an increasing role and then a pure elastic transmission cannot catch all the transport physics. Implicit in this approach is the assumption that the shortest time scale of the problem is provided by the propagating charge, so that the time dependence can be considered as a pure parametric one. In this latter case, the model equation (5) seems to us more appropriate,

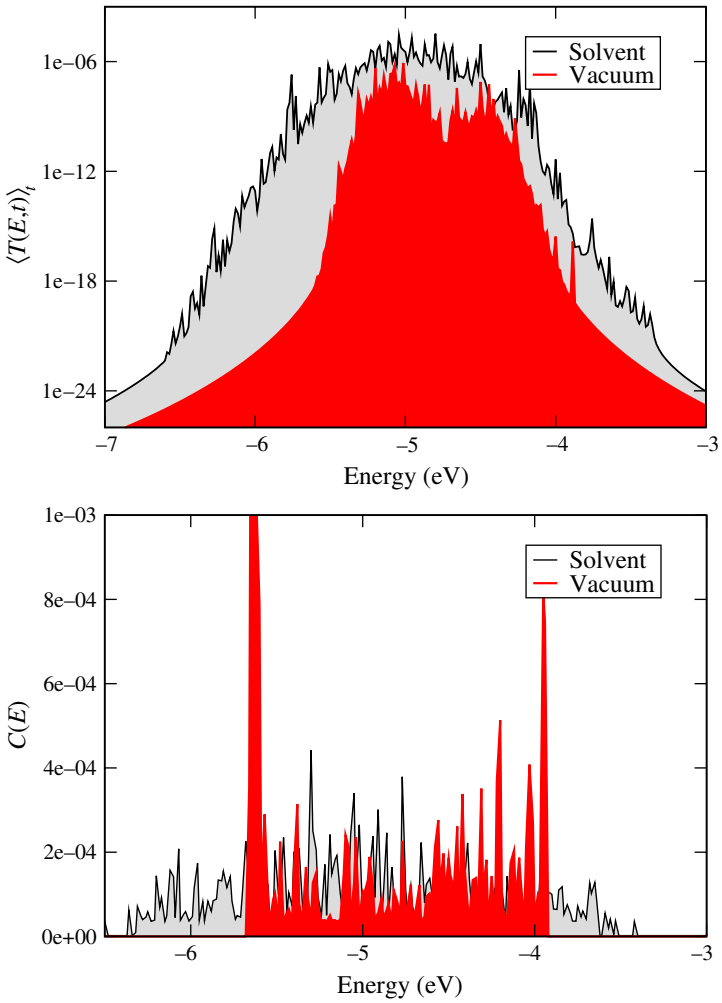

Figure 3. Upper panel: time-averaged transmission function for simulations performed in the solvent and in vacuum. Lower panel: coherence parameter $C(E)$ for the DD in the solvent and in vacuum. Note that the influence of the solvent fluctuations is to spread out the spectral support of $C(E)$. As expected, the coherence parameter is on average larger for the vacuum case where a large part of the fluctuations is suppressed due to the absence of an environment. Nevertheless the transmission in the vacuum case is much smaller, nicely illustrating the positive influence of the environment in gating charge migration.

since it includes the dressing of the electronic degrees of freedom by the structural fluctuations. In figure 3, we show the averaged transmission function (upper panel) for the cases where solvent effects are included or neglected, respectively. We clearly see that solvent-mediated fluctuations considerably increase and broaden the transmission spectrum. Its fragmented structure is simply due to the fluctuations in the on-site energies, which make the system effectively highly disordered. Another way of looking at the effect of fluctuations is via the introduction of a coherence parameter [36], which is defined as $C(E) = \langle T(E,t)\rangle_t^2 / \langle T(E,t)^2\rangle_t$. If the fluctuations are weak $C(E)$ goes to one, while a strongly fluctuating system will lead to

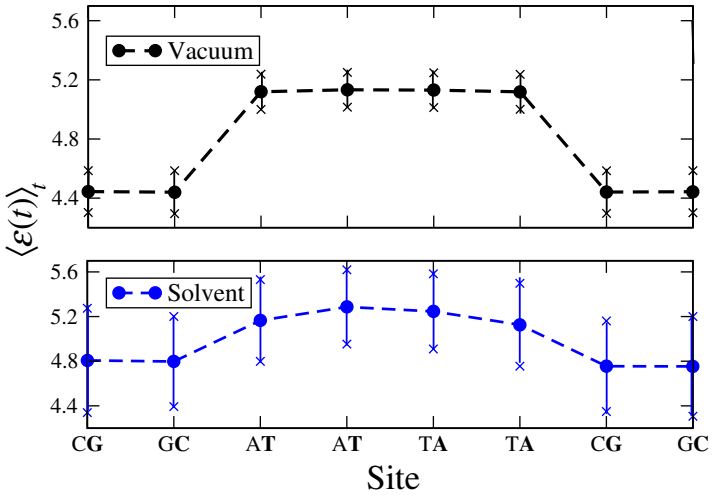

Figure 4. Time average of the absolute value of the on-site energies along the segment covering bases 3 and 10 of the DD, i.e. over the sequence 5′-CGAATTCG-3′) for simulations in vacuum (upper panel) and in the solvent (lower panel). The outermost two bases on each end were not included in the calculations to avoid undesired boundary effects. The averaged energy profile in the presence of the solvent becomes smoother, but also the fluctuations around the averages are stronger. This smoothing reduces the energy barriers between the sites and hence favors charge migration.

a considerable reduction of $C(E)$. Obviously, this parameter has only a clear meaning for the spectral support of the transmission function. $C(E)$ is shown in the lower panel of figure 3; the coherence parameter in vacuum conditions can become larger than in the solvent for some small energy regions due to the reduction of the fluctuations. However, this does not turn out to be enough to increase the transport efficiency for the special base sequence of the Dickerson DNA, since this system has in the static limit a distribution of energetic barriers due to the base pair sequence. To further illustrate the influence of the solvent, we have plotted in figure 4 the time-averaged on-site energies along the model tight-binding chain. Remarkably, the presence of the solvent 'smoothes' the averaged energy profile (although the amplitude of fluctuations clearly becomes stronger). To compute the current through the system, we use the Hamiltonian equation (5) and the current expression, equation (8), derived with this model. The Fermi energy in these calculations was fixed at the upper edge of the transmission spectrum (see figure 3). The qualitative results, however, are not considerably changed by slightly changing its position. In figure 5, the current is shown for the two cases of interest. Due to the presence of tunnel barriers in the wire, which are not fully compensated on average by the gating effect of the environment, the absolute current values are rather small when compared with those of homogeneous sequences [36]. However, the current including the solvent is roughly 15 times larger than that obtained from the simulations in vacuum. Although our model Hamiltonian in equation (5) does not fully contain all the dynamical correlations encoded in the time-dependent electronic parameters, we nevertheless expect that their inclusion would lead to an even further increase of the difference between the solvent and vacuum results, thus supporting our main conclusions.

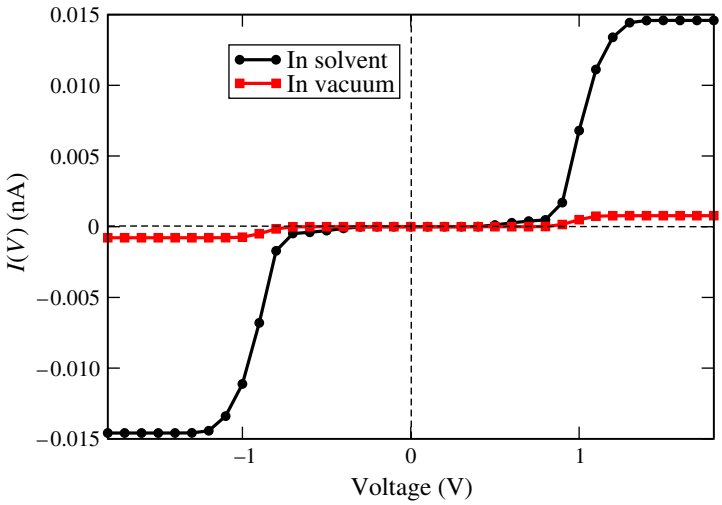

Figure 5. Electrical current for the DD in both vacuum (no solvent) and including the solvent. The current is considerably enhanced upon inclusion of solvent fluctuations, nicely demonstrating the strong gating effect of the latter on the energy profile of the DNA chain.

3. Conclusions

We have presented a hybrid methodology that allows for a very efficient coarse-graining of the electronic structure of complex biomolecular systems and allows us to include the influence of structural fluctuations in the electronic parameters. The time series obtained in this way allow us to map the problem onto an effective low-dimensional model Hamiltonian describing the interaction of charges with a bosonic bath, which comprises the dynamical fluctuations. The possibility to parameterize the bath spectral density $J(\omega)$ using the information obtained from the time series makes our approach very efficient, since we do not need to use the typical phenomenological ansatze (ohmic, Lorentzian, etc) to describe the bath dynamics. The example presented here, the DD, clearly shows that solvent-mediated gating may be a very efficient mechanism supporting charge transport if the static DNA reference structure already possesses a disordered energy profile (due to the base sequence). Our method is obviously not limited to the treatment of DNA, but it can equally well be applied to deal with charge migration in other complex systems like molecular organic crystals or polymers, where charge dynamics and coupling to fluctuating environments play an important role [62]–[64], [79]–[83].

Acknowledgments

We acknowledge Florian Pump for fruitful discussions. This work was supported by the Deutsche Forschungsgemeinschaft (DFG) within the Priority Program 1243 'Quantum transport at the molecular scale' under contract CU 44/5-2, by the Volkswagen Foundation through grant no. I/78-340, by the European Union under contract IST-029192-2, by the cluster of excellence of the Free State of Saxony 'European Center for Emerging Materials and Processes Dresden' ECEMP/A2, by the ESF project innovaSens and by WCU (World Class University) program, through the Korea Science and Engineering Foundation funded by the Ministry of Education,

Science and Technology (Project no. R31-2008-000-10100-0). We also acknowledge the Center for Information Services and High Performance Computing (ZIH) at Dresden University of Technology for computational resources.

References

[1] Braun E, Eichen Y, Sivan U and Ben-Yoseph G 1998 *Nature* **391** 775
[2] Porath D, Bezryadin A, Vries S D and Dekker C 2000 *Nature* **403** 635
[3] Cohen H, Nogues C, Naaman R and Porath D 2005 *Proc. Natl Acad. Sci. USA* **102** 11589
[4] Xu B, Zhang P, Li X and Tao N 2004 *Nano Lett.* **4** 1105
[5] Yoo K-H, Ha D H, Lee J-O, Park J W, Kim J, Kim J J, Lee H-Y, Kawai T and Choi H Y 2001 *Phys. Rev. Lett.* **87** 198102
[6] Porath D, Cuniberti G and Felice R D 2004 *Long-Range Charge Transfer in DNA I and II (Topics in Current Chemistry* vol 237*)* ed G B Schuster (Berlin: Springer) p 183
[7] *Modern Methods for Theoretical Physical Chemistry of Biopolymers* 2006 ed S Tanaka, J Lewis and E Starikow (Amsterdam: Elsevier)
[8] *NanoBioTechnology: BioInspired Device and Materials of the Future* 2007 ed O Shoseyov and I Levy (Humana Press)
[9] *Charge Migration in DNA: Perspectives from Physics, Chemistry and Biology* 2007 ed T Chakraborty (Berlin: Springer)
[10] Roche S 2003 *Phys. Rev. Lett.* **91** 108101
[11] Cuniberti G, Craco L, Porath D and Dekker C 2002 *Phys. Rev.* B **65** 241314
[12] Shih C-T, Roche S and Romer R A 2008 *Phys. Rev. Lett.* **100** 018105
[13] Guo A-M and Xiong S-J 2009 *Phys. Rev.* B **80** 035115
[14] Meggers E, Michel-Beyerle M E and Giese B 1998 *J. Am. Chem. Soc.* **120** 12950
[15] Meggers E, Kusch D, Spichty M, Wille U and Giese B 1998 *Angew. Chem. Int. Edn Engl.* **37** 460
[16] Treadway C R, Hill M G and Barton J K 2002 *Chem. Phys.* **281** 409
[17] Turro N J and Barton J K 1998 *J. Biol. Inorg. Chem.* **3** 201
[18] Wan C, Fiebig T, Kelley S O, Treadway C R and Barton J K 1999 *Proc. Natl Acad. Sci. USA* **96** 6014
[19] O'Neill M A and Barton J K 2004 *J. Am. Chem. Soc.* **126** 11471
[20] Henderson P T, Jones D, Hampikian G, Kan Y and Schuster G B 1999 *Proc. Natl Acad. Sci. USA* **96** 8353
[21] Grozema F C, Tonzani S, Berlin Y A, Schatz G C, Siebbeles L D and Ratner M A 2008 *J. Am. Chem. Soc.* **130** 5157
[22] Grozema F, Berlin Y and Siebbeles L D A 2000 *J. Am. Chem. Soc.* **122** 10903
[23] Troisi A and Orlandi G 2002 *J. Phys. Chem.* B **106** 2093
[24] Senthilkumar K, Grozema F C, Guerra C F, Bickelhaupt F M, Lewis F D, Berlin Y A, Ratner M A and Siebbeles L D A 2005 *J. Am. Chem. Soc.* **127** 148094
[25] Barnett R N, Cleveland C L, Joy A, Landman U and Schuster G B 2001 *Science* **294** 567
[26] Chaudhury S and Cherayila B J 2007 *J. Chem. Phys.* **127** 145103
[27] Wang H, Lin S, Allen J P, Williams J C, Blankert S, Laser C and Woodbury N W 2007 *Science* **316** 747
[28] Min W and Xie X S 2006 *Phys. Rev.* E **73** 010902
[29] Lu H P, Xun L and Xie X S 1998 *Science* **282** 1877
[30] Wennmalm S, Edman L and Rigler R 1999 *Chem. Phys.* **247** 61
[31] Kim J, Doose S, Neuweiler H and Sauer M 2006 *Nucl. Acids Res.* **34** 2516
[32] Hihath J, Xu B Q, Zhang P M and Tao N J 2005 *Proc. Natl Acad. Sci. USA* **102** 16979
[33] Hennig D, Starikov E B, Archilla J F R and Palmero F 2004 *J. Biol. Phys.* **30** 227
[34] Yamada H, Starikov E and Hennig D 2007 *Eur. Phys. J.* B **59** 185
[35] Cramer T, Krapf S and Koslowski T 2007 *J. Phys. Chem.* C **111** 8105

[36] Gutierrez R, Caetano R, Woiczikowski P B, Kubar T, Elstner M and Cuniberti G 2009 *Phys. Rev. Lett.* **102** 208102
[37] Woiczikowski P B, Kubar T, Gutierrez R, Caetano R, Cuniberti G and Elstner M 2009 *J. Chem. Phys.* **130** 215104
[38] Gutierrez R, Mandal S and Cuniberti G 2005 *Nano Lett.* **5** 1093
[39] Gutierrez R, Mandal S and Cuniberti G 2005 *Phys. Rev.* B **71** 235116
[40] Schmidt B B, Hettler M H and Schön G 2007 *Phys. Rev.* B **75** 115125
[41] Schmidt B B, Hettler M H and Schon G 2008 *Phys. Rev.* B **77** 165337
[42] Voityuk A, Rösch N, Bixon M and Jortner J 2000 *J. Phys. Chem.* B **104** 5661
[43] Voityuk A A 2008 *J. Chem. Phys.* **128** 115101
[44] Voityuk A A 2005 *J. Chem. Phys.* **123** 034903
[45] Mehrez H and Anantram M P 2005 *Phys. Rev.* B **71** 115405
[46] Calzolari A, Felice R D, Molinari E and Garbesi A 2002 *Appl. Phys. Lett.* **80** 3331
[47] Felice R D, Calzolari A and Molinari E 2002 *Phys. Rev.* B **65** 045104
[48] Felice R D, Calzolari A and Zhang H 2004 *Nanotechnology* **15** 1256
[49] Lewis J P, Cheatham T E, Starikov E B, Wang H and Sankey O F 2003 *J. Phys. Chem.* B **107** 2581
[50] Ladik J, Bende A and Bogar F 2008 *J. Chem. Phys.* **128** 105101
[51] Drew H, Wing R, Nakano T, Broka C, Tanaka S, Itakura K and Dickerson R E 1981 *Proc. Natl Acad. Sci. USA* **78** 2179
[52] Kubar T, Woiczikowski P B, Cuniberti G and Elstner M 2008 *J. Phys. Chem.* B **112** 7937
[53] Kubar T and Elstner M 2008 *J. Phys. Chem.* B **112** 8788
[54] Song B, Elstner M and Cuniberti G 2008 *Nano Lett.* **8** 3217
[55] Gutierrez R, Mohapatra S, Cohen H, Porath D and Cuniberti G 2006 *Phys. Rev.* B **74** 235105
[56] Voityuk A A, Siriwong K and Rösch N 2004 *Angew. Chem. Int. Edn Engl.* **43** 624
[57] Cui Q, Elstner M, Kaxiras E, Frauenheim T and Karplus M 2001 *J. Phys. Chem.* B **105** 569
[58] Kenkre V M and Brown D W 1985 *Phys. Rev.* B **31** 2479
[59] Kenkre V M and Schmid D 1985 *Phys. Rev.* B **31** 2430
[60] Haken H and Reineker P 1972 *Z. Phys.* A **249** 253
[61] Kühne R and Reineker P 1975 *Z. Phys.* B **22** 201
[62] Skourtis S S, Balabin I A, Kawatsu T and Beratan D N 2005 *Proc. Natl Acad. Sci. USA* **102** 3552
[63] Gudowska-Nowak E 1996 *Chem. Phys.* **212** 115
[64] Goychuk I A, Petrov E G and May V 1995 *J. Chem. Phys.* **103** 4937
[65] Damjanovic A, Kosztin I, Kleinekathöfer U and Schulten K 2002 *Phys. Rev.* E **65** 031919
[66] Berlin Y A, Grozema F C, Siebbeles L D A and Ratner M A 2008 *J. Phys. Chem.* C **112** 10988
[67] Berlin Y A, Burin A L and Fischer S F 1997 *Chem. Phys.* **220** 25
[68] Mahan G D 2000 *Many-Particle Physics* 3rd edn (New York: Plenum)
[69] Galperin M, Nitzan A and Ratner M A 2006 *Phys. Rev.* B **73** 045314
[70] Weiss U 1999 *Quantum Dissipative Systems* (*Series in Modern Condensed Matter Physics* vol 10) (Singapore: World Scientific)
[71] Meir Y and Wingreen N S 1992 *Phys. Rev. Lett.* **68** 2512
[72] Grabert H and Devoret M H (ed) 1992 *Proc. NATO ASI on Single Charge Tunneling (Les Houches, March 1991)* (New York: Plenum)
[73] Kubo R 1962 *J. Phys. Soc. Japan* **17** 1100
[74] Wang J, Cieplak P and Kollman P A 2000 *J. Comput. Chem.* **21** 1049
[75] Perez A, Marchan I, Svozil D, Sponer J, Cheatham T E III, Laughton C A and Orozco M 2007 *Biophys. J.* **92** 3817
[76] van der Spoel D, Lindahl E, Hess B, Groenhof G, Mark A E and Berendsen H J C 2005 *J. Comput. Chem.* **26** 1701
[77] Lu X and Olson W K 2003 *Nucl. Acids Res.* **31** 5108

[78] http://structure.usc.edu/make-na/server.html
[79] Troisi A, Cheung D L and Andrienko D 2009 *Phys. Rev. Lett.* **102** 116602
[80] Soules T F and Duke C B 1971 *Phys. Rev.* B **3** 262
[81] Andrews D Q, Van Duyne R P and Ratner M A 2008 *Nano Lett.* **8** 1120
[82] Troisi A, Ratner M A and Zimmt M B 2004 *J. Am. Chem. Soc.* **126** 2215
[83] Bicout D J and Field M J 1995 *J. Phys. Chem.* **99** 12661
[84] Malen J A, Doak P, Baheti K, Don T Tilley, Majumdar A and Segalman R A 2009 *Nano Lett.* **9** 3406
[85] Berlin Y A, Burin A L, Siebbeles L D A and Ratner M A 2001 *J. Phys. Chem.* A **105** 5666